Journal of Photochemistry & Photobiology, A: Chemistry 448 (2024) 115318

Contents lists available at ScienceDirect

Journal of Photochemistry & Photobiology, A: Chemistry

journal homepage: www.elsevier.com/locate/jphotochem

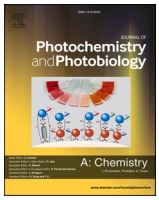

Green synthesis of silver nanoparticles (AgNPs) by *Lallemantia royleana* leaf Extract: Their Bio-Pharmaceutical and catalytic properties

Majid Sharifi-Rad [a,*], Hazem S. Elshafie [b], Pawel Pohl [c]

[a] *Department of Range and Watershed Management, Faculty of Water and Soil, University of Zabol, Zabol 98613-35856, Iran*
[b] *School of Agricultural, Forestry, Food and Environmental Sciences, University of Basilicata, Viale dell'Ateneo Lucano 10, 85100 Potenza, Italy*
[c] *Department of Analytical Chemistry and Chemical Metallurgy, Faculty of Chemistry, Wroclaw University of Science and Technology, Wyspianskiego 27, 50-370 Wroclaw, Poland*

ARTICLE INFO

Keywords:
Green nanoparticle
Nanotechnology
Biological applications
Catalytic application
Antimicrobial activity

ABSTRACT

The study of the silver nanoparticles (AgNPs) synthesis based-green methods become more interesting recently due to their low-cost preparation, eco-friendly and non-toxic precursors. The present study approved the ability of the *Lallemantia royleana* (Benth. in Wall.) Benth. leaf extract for the synthesis of AgNPs for the first time. The synthesized AgNPs were physico-chemical characterized using ultraviolet–visible spectroscopy (UV–Vis), X-ray diffraction (XRD), Fourier Transform-Infrared Spectroscopy (FT-IR), zeta potential and transmission electron microscopy (TEM) analysis. The total phenols, flavonoids, anthocyanin, tannin contents, antioxidant, antimicrobial, anti-inflammatory, anti-arthritic and cytotoxic activities of *L. royleana* leaf extract and the synthesized AgNPs were investigated. The biocatalytic activity of prepared AgNPs was assessed on methylene blue as a pollutant organic dye. The TEM examination showed that the synthesized AgNPs were predominantly spherical with some mixed shapes and crystalline with average size 34.47 ± 1.6 nm, and showed a localized surface plasmon resonance (LSPR) peak at 425 nm. The zeta potential value was −24.1 mV indicating the stability of produced AgNPs. The new prepared AgNPs have lower total phenols, flavonoids, anthocyanin, tannin contents than *L. royleana* leaf extract. In addition, the new prepared AgNPs demonstrated the higher DPPH radical scavenging activity (87 %) and the ABTS radical scavenging activity (77 %) at the maximum prepared concentration of 250 μg mL^{-1} as compared to the *L. royleana* leaf extract (62 % and 58 %, respectively). The produced AgNPs also exhibited the higher antimicrobial activity against both the Gram-positive (*Staphylococcus aureus* and *Bacillus cereus*) and the Gram-negative (*Escherichia coli* and *Shigella flexneri*) bacteria and the *Candida* strains (*Candida glabrata and Candida albicans*) as compared to the *L. royleana* leaf extract. The resulting AgNPs indicated a dose-dependent anti-inflammatory effect on human red-blood cell (RBC) membrane stabilization assay and had more activity (72 %) compared to the *L. royleana* leaf extract (61 %) at 250 μg mL^{-1}. The prepared AgNPs showed promising *in vitro* anti-arthritic activity evaluated by 73 % compared to 58 % in case of *L. royleana* leaf extract. The new produced AgNPs showed the higher cytotoxic effect against the human hepatoma (Hep-G2) and the human breast (MCF-7) cancer cells compared to the *L. royleana* leaf extract with 79.3 % and 77.2 % at 250 μg/mL, respectively. The obtained results revealed also that the green synthesized AgNPs were capable to catalyze MB dye. Therefore, the obtained results provide a promising route of the green synthesis of AgNPs using *L. royleana* leaf extract with considerable biopharmaceuticals and catalytic applications.

1. Introduction

Nanotechnology is defined as the manipulation of materials with dimensions sized from 1 to 100 nm for numerous fields of applications, such as: medical, electronics, energy production, and consumer goods [1,2]. The framework for incorporating and regulating molecules as well as atoms is provided by the nanoscale material generation [3]. The interdisciplinary subject of nanobiotechnology is expanding quickly and has different practical applications in medicine, agriculture and industry [4,5]. Many plants and microbes in particular have drawn significant interest as useful resources for the nanomaterials synthesis [6] due to their nontoxicity, eco-friendliness, and safety. In addition, the

* Corresponding author.
E-mail address: majidsharifirad@uoz.ac.ir (M. Sharifi-Rad).

https://doi.org/10.1016/j.jphotochem.2023.115318
Received 5 September 2023; Received in revised form 1 November 2023; Accepted 3 November 2023
Available online 8 November 2023

nanoparticles (NPs) generated with the aid of bacteria, fungi, and plants are more desirable than those made with the aid of chemical agents, especially when considering their prospective usage in food goods and medications [4,7,8].

NPs of metals like silver (Ag), gold (Au), platinum (Pt), copper (Cu), zinc (Zn), titanium (Ti), and magnesium (Mg) have attracted a lot of attention especially considering their biomedical applications due to their versatile theragnostic properties [9].

Silver nanoparticles (AgNPs) are more and more popular especially in biomedicines because their broad antimicrobial activity is very helpful in the developed drug delivery systems [10]. A possible mode of action of AgNPs is correlated to their hydrophilic - hydrophobic balance and a target specific localized surface resonance (LSR) characteristic, which offers a variety of chances for the drug delivery and modification systems [11,12].

Among various biosynthesized metallic NPs, AgNPs are emerged as the champion in the last two decades due to their unique biological, chemical, and physical properties [13]. Although Ag is toxic at higher concentrations, many studies have established that this element in the form of AgNPs and at a lower concentration has the desired chemical stability, the high catalytic activity, the good biocompatibility, and the intrinsic therapeutic potential [9]. AgNPs are also reported to have the anticancer and antimicrobial activity [14]. In fact, a slow and regulated release of Ag from AgNPs is one of the most striking advantages of these NPs when compared with the bulk metal and their salts [15]. A combination of nanotechnology and traditional medicine is the mantra of the new-age bio-nanoformulations.

In particular, AgNPs are synthesized *via* a variety of processes, including electrochemical and photochemical reductions, heat evaporation, and biological techniques [3]. However, these conventional techniques are extremely costly and also involve the use of dangerous chemicals which cause many threats to the human health and the environment. Therefore, the synthesis of AgNPs based on the natural sources such as microbial and plant extracts is receiving a great attention because they are cheaper and environmentally friendly [16].

Gengan et al. [14] reported that the plant-mediated synthesis of metallic NPs is also gaining on popularity due to its low time requirement and high efficacy. On the other hand, plants are a rich natural source of bioactive secondary metabolites, such as terpenoids, polysaccharides, phenolic compounds and alkaloids, which can be utilized as reducing agents for the conversion of the metal ions to their reduced forms, resulting in the production of the NPs with the predetermined size and properties [15,17].

Lallemantia royleana (Benth. In Wall.) is a species of a flowering plant of the *Lamiaceae* family. It is an endemic mucilaginous plant that is widely cultivated in various parts of Europe and Middle East, in particular Turkey, Iran and India [18]. In Iran, *L. royleana* is known as balangu shirazi and used as a folk medicine to treat fever and coughs [19]. In Iran and Turkey, its seeds are utilized in a variety of conventional or modern items, including the ingredients of beverages and bread [20], because they are a good source of polysaccharides, fibers, oils, and proteins [21]. Particularly, the balangu seed-mucilage is made up of 296.6 g of crude fibers, 83.3 g of ash, and 617.4 g of carbohydrates per kilogram of seeds [22].

Considering the importance of the synthesis of the biogenic AgNPs that can have specific bio-pharmaceutical and catalytic activities, the main aim of the current research was to develop the new green synthesis procedure of AgNPs using the ethanolic *L. royleana* leaf extract. In addition, the obtained AgNPs were characterized using ultraviolet–visible spectroscopy (UV–Vis), Fourier-transform infrared spectroscopy (FT-IR), X-ray diffraction (XRD), transmission electron microscopy (TEM), and the zeta potential analysis. Furthermore, the following bio-pharmaceutical properties of the obtained AgNPs, i.e., antioxidant, antimicrobial and anti-inflammatory, were also investigated. To the best of our knowledge, this is the first study on the green synthesis of AgNPs by the ethanolic *L. royleana* leaf extract.

2. Materials and methods

2.1. Chemicals and reagents

All chemicals and reagents used in this research were purchased from Sigma-Aldrich (>99 % purity).

2.2. Plant material

Samples of the *L. royleana* leaves were obtained in May 2022 from the Fars province rangelands, Iran. The plant material was botanically authenticated at the Department of Rangeland and Watershed Management, University of Zabol, Zabol, Iran, where a voucher specimen (No. 58421) was deposited. The collected leaves were first cleaned with tap water, air dried in shading, and processed in a blender to obtain a fine powder. The resulting leaf powder was treated with ethanol (98 %) (20 mL/g) and shaked for 24 h at room temperature. The resultant ethanolic extract was filtered using a filter paper (Whatman No. 1). The filtrate was kept in dark in a refrigerator at 4 °C. In addition, the ethanolic extract was also evaporated to dryness using a rotary evaporator under a reduced pressure at 20–30 °C, and stored in dark at 4 °C for further analysis.

2.3. Green synthesis of AgNPs

AgNPs were synthesised by mixing an aqueous solution of the ethanolic *L. royleana* leaf extract with a solution of silver nitrate ($AgNO_3$; 1 mmol/L) at ratio 1:9, as reported by Sharifi-Rad et al [4]. The synthesis was carried out by continuously shaking the reaction mixture at room temperature for 150 min. Finally, the suspension was centrifuged at 20,000 rpm for 15 min. The resulting pellet was cleaned twice with Milli-Q water (MQW) to get rid of the residue of the plant extract and the precursor of AgNPs. Finally, it was left for air-drying at room temperature. For further analysis, the resulting AgNPs were suspended in MQW to get their suspensions at various concentrations.

2.4. Physicochemical characterization of synthesized AgNPs

2.4.1. Uv–vis absorption spectrophotometry

The presence of the green-synthesized AgNPs in the resulting reaction mixtures was proved by using UV–Vis absorption spectrophotometry (UV-1800, Shimadzu Corporation, Kyoto, Japan). The UV–Vis absorption spectra of these mixtures, obtained after various time intervals, were acquired in the range from 300 to 800 nm. MQW was used as a blank for zeroing the spectrophotometer.

2.4.2. FT-IR spectroscopy

For FT-IR spectroscopy, a Nicolet 800 FTIR spectrometer (Nicolet, Madison, WI, USA) was used to identify the functional groups of the chemical species present in the dried *L. royleana* leaf extract as well as those chemical species that capped and stabilized the produced AgNPs. The biomolecules present in the ethanolic *L. royleana* leaf extract, involved in the reduction of the Ag(I) ions, were identified in the frequency range of 500 to 4000 cm^{-1} according to the KBr pellet method [23,24].

2.4.3. X-ray diffraction

A Siemens X-ray diffractometer (XRD), model D5000 (Munich, Germany), with a 0.5-min dwell period, was used to acquire the crystallinity and X-ray diffraction pattern of the dried AgNPs. Using a Cu–Kα radiation (λ = 1.54 Å) lamp, appropriate diffractograms of the AgNPs were obtained over the scanning range of the 2theta angle, changing from 20 to 80° [13]. The average crystallite size of the synthesized AgNPs was determined using the Debye-Scherrer's formula as reported by Manik et al. [13].

2.4.4. TEM examination for the particles size and distribution

A transmission electron microscopy (TEM) instrument, model Philips GM-30 (Hillsboro, OR, USA), running at a 120 kV accelerating voltage, was used to investigate the morphology and the size of the AgNPs, as explained by Sharifi-Rad et al. [4]. Briefly, the obtained AgNPs were suspended in MQW and sonicated for 5 min. A drop (50 μL) of the resultant suspension was deposited on a carbon-coated copper grid and the solvent was evaporated under the light of an infra-red (IR) lamp for 15 min. Digimizer software (Version 5.4.3, MedCalc Software, Ostend, Belgium) was used to assess the morphology of the AgNPs and determine their particles size and the size distribution. In addition, the zeta potential of the AgNPs was assessed at 25 °C using a Zetasizer Nano ZS instrument (Nano-ZS; Malvern Instruments Ltd., Worcestershire, UK).

2.5. Phytochemical screening

To investigate the presence of and quantity of the important non-nutritional bioactive compounds in the *L. royleana* leaf extract and the new synthesized AgNPs, some essential phytochemical analyses were carried out according to Sharifi-Rad et al. [25]:

2.5.1. Total phenolic compounds concentration

The total phenolic compounds (TPC) concentration was determined using the Folin–Ciocalteu reagent as described by Dewanto et al. [26]. Briefly, the studied plant extract or the synthesized AgNPs were separately dissolved/dispersed in MQW until the desired final concentration was achieved (25, 50, 100, 150, 200, 250 μg mL^{-1}). 1 mL of such prepared solutions of the studied plant extract or dispersions of the synthesized AgNPs was mixed with 5 mL of a 10 % (w/v) Folin–Ciocalteu reagent solution. Then, 4 mL of a 5 % (w/v) Na_2CO_3 solution was added. Each final mixture was kept in darkness at room temperature for 2 h, next, its absorbance was measured at 760 nm using a UV–Vis spectrophotometer (UV-1800, Shimadzu Corporation, Kyoto, Japan). The TPC was expressed in milligrams of the gallic acid equivalent per gram of dry weight of the plant extract or the AgNPs (mg GAE/g dry weight). The gallic acid standards (the concentration range of the standard solutions 25–250 μg mL^{-1}, $y = 0.0086x - 0.0002$, $R^2 = 0.994$) were measured at the same operating conditions for the standard calibration.

2.5.2. Total flavonoid compounds concentration

The method developed by Chang et al. [27] was used to measure the total concentration of flavonoid compounds (TFC). Briefly, 0.5 mL of the solutions of the studied plant extract or the dispersions of the synthesized AgNPs, both at concentrations of 25, 50, 100, 150, 200, and 250 μg mL^{-1}, was separately mixed with 1.5 mL of methanol, 0.1 mL of a potassium acetate solution (1 mol/L), 0.1 mL of a $AlCl_3$ solution (10 %), and 2.8 mL of MQW. The resultant mixtures were left at room temperature for 30 min. Their absorbance was measured then at 415 nm with a Shimadzu UV-1800 UV–Vis spectrophotometer. A calibration curve was used to quantitatively determine the TFC as milligrams of the quercetin equivalent per gram of dry weight of the plant extract or the AgNPs (mg QE/g dry weigh). The concentration of quercetin in the standards was within 25–250 μg mL^{-1} ($y = 0.0094x - 0.036$, $R^2 = 0.995$).

2.5.3. Total anthocyanins concentration

Using the pH differential approach described by Vega-Arroy et al. [28], the concentration of all anthocyanins (TAC) was determine as here described. 10 mL of the solutions of the studied plant extract or the suspensions of the synthesized AgNPs, both at concentrations of 25, 50, 100, 150, 200, and 250 μg mL^{-1}, were mixed with 1 mol/L HCl or 1 mol/L NaOH solutions to reach pH of 1 or 4.5, respectively. Finally, the absorbance of such prepared solutions was measured at 520 and 700 nm, respectively, using a Shimadzu UV-1800 UV–Vis spectrophotometer. Cyanidin-3-glucoside was used as the standard for the calibration (the concentration range of the standard solutions 25–250 μg mL^{-1}, $y = 0.0203x + 0.0166$, $R^2 = 0.993$). The equations (1) and (2) were used to calculate the TAC, expressed as the cyanidin-3-glucoside equivalent (in mg/100 g of the dry weight of the plant extract or the AgNPs):

$$A = (A_{520\ nm} - A_{700\ nm})_{pH\ \ 1.0} - (A_{520\ nm} - A_{700\ nm})_{pH\ 4.5} \quad (1)$$

$$The\ TAC(mg/100g) = (A \times MW \times DF \times 1000)/\varepsilon \times 1 \quad (2)$$

where A is the difference in the absorbance acquired at different pHs; MW (molecular weight) = 449.2 g mol^{-1} of cyanidin-3-glucoside; DF is the dilution factor; 1 = quartz cell pathway (1 cm); and ε is the molar extinction coefficient for cyanidin-3-glucoside (26,900 M^{-1} cm^{-1}).

2.5.4. Total tannins concentration

The total tannins concentration (TTC) was determined following the method described by Sun et al. [29]. Briefly, 50 μL of the solutions of the studied plant extract or the suspensions of the synthesized AgNPs, both at concentrations of 25, 50, 100, 150, 200, and 250 μg mL^{-1}, was mixed with 2 mL of a vanillin solution (4 %) in methanol and 1.5 mL of concentrated HCl. Then, after 25 min, the absorbance of the prepared mixtures was measured at 500 nm using a Shimadzu UV-1800 UV–Vis spectrophotometer. The standard for the calibration used was catechin (the concentration range of the standard solutions 25–250 μg mL^{-1}, $y = 0.0038x + 0.0014$, $R^2 = 0.995$), while methanol was employed as the blank. The TTC was expressed in mg of catechin/g dry weight of the plant extract or AgNPs.

2.6. Antioxidant assay

2.6.1. DPPH (2,2-diphenyl-1-picrylhydrazyl) radical scavenging activity test

The DPPH radical scavenging activity of the *L. royleana* leaf extract and the synthesized AgNPs was expressed as the inhibition percentage in the DPPH radical and evaluated according to the method described by Sharifi-Rad *et al.* [4]. In summary, 0.4 mL of the solutions of the *L. royleana* leaf extract and the suspensions of the green-synthesized AgNPs, both at concentrations of 25, 50, 100, 150, 200, and 250 μg mL^{-1}, were mixed with 3 mL of a 0.1 mmol/L DPPH radical working solution. The resulting reaction mixtures were kept at a room temperature for 30 min, and after that, the absorbance of the prepared samples solutions was measured at 517 nm using a Shimadzu UV-1800 UV–Vis spectrophotometer. The solutions of butylated hydroxyanisole (BHA) at the same concentrations as in the case of the suspensions of AgNPs and the *L. royleana* leaf extract solutions were used as the positive controls. The DPPH radical working solution was used as the negative control. The radical scavenging activity percentage (RSA %) was determined using the formula (1):

$$RSA(\%) = \left[\left(A_{control} - A_{sample}\right)/A_{control}\right] \times 100 \quad 1)$$

where: $A_{control}$ is the absorbance of the control (DPPH); A_{sample} is the absorbance of the tested sample.

2.6.2. $ABTS^{\bullet+}$ (2,20-azino-bis(3-ethylbenzothiazoline-6-sulfonic acid)

The ABTS radical scavenging activity of the *L. royleana* leaf extract and the synthesized AgNPs was expressed as the percentage inhibition in the ABTS radical and evaluated according to Min-Jung et al. [30]. The working solution of ($ABTS^{\bullet+}$) was made by mixing an equal amount of both $ABTS^{\bullet+}$ (7.0 mmol L^{-1}) and potassium persulfate solution ($K_2S_2O_8$) (2.4 mmol/L), which was then left at room temperature and in dark for 16 h. 100 μL of the *L. royleana* leaf extract solutions or 100 μL of synthesized AgNPs suspensions, both at concentrations of 25, 50, 100, 150, 200, and 250 μg mL^{-1}, were separately added to the ABTS radical working solution (3 mL). The solutions of BHA at the same concentrations as in the case of the suspensions of AgNPs and the *L. royleana* leaf extract solutions were used as the positive controls. The absorbance of the resulting samples solutions was measured at 734 nm after 30 min, using a Shimadzu UV–Vis spectrophotometer, model UV-1800, against a

respective negative control, i.e., the ABTS radical working solution. The RSA (%) was determined following the Formula (1) as above-explained.

2.7. Antibacterial assays

The antibacterial activity of the *L. royleana* leaf extract and the synthesized AgNPs was assessed against the following bacteria strains: *Staphylococcus aureus* (ATCC: 25923), *Bacillus cereus* (ATCC: 11778), *Escherichia coli* (ATCC: 25922), and *Shigella flexneri* (ATCC: 12022), which were obtained from the Iranian Research Organization for Science and Technology (IROST).

2.7.1. Minimum inhibitory concentration (MIC)

The Clinical and Laboratory Standards Institute's (CLSI) recommendations [30] were followed to establish the minimum inhibitory concentration (MIC) of the *L. royleana* leaf extract and the synthesized AgNPs. The solutions of the leaf extract and the suspensions of AgNPs, both at concentrations within the range from 300 to 2.35 μg mL^{-1}, were prepared. The Müller-Hinton broth (50 μL) and variously concentrated solutions of the *L. royleana* leaf extract (50 μL) were added into each well of a Microplate-96 plate. Using another microplate-96 plate, the Müller-Hinton broth (50 μL) and variously concentrated suspensions of the synthesized AgNPs were added to the wells. Finally, 50 μL of the prepared bacterial suspensions (10^8 CFU mL^{-1}) were added to each well of the plate. Then, the inoculation plates were incubated at 37 °C for 24 h. The MIC values described the lowest concentrations of the *L. royleana* leaf extract and the synthesized AgNPs that entirely prevented each tested bacterium strain from its visible growth.

2.7.2. Minimum bactericidal concentration (MBC)

The Clinical and Laboratory Standards Institute's (CLSI) recommendations [31] were followed to determine the minimum bactericidal concentration (MBC) of the *L. royleana* leaf extract and the synthesized AgNPs. Briefly, 50 μL from each well of the broth micro-dilution test that showed no observable bacterial growth was taken and spread on the Müller-Hinton agar (MHA) plates. Then, the plates were incubated at 37 °C for 24 h. The lowest concentration that showed no observable bacterial growth after this sub-culturing was considered as the MBC.

2.8. Antifungal activity

The antifungal activity of the *L. royleana* leaf extract and the synthesized AgNPs was evaluated against the standard *Candida* strains: *Candida glabrata* (ATCC 90030) *and Candida albicans* (ATCC 14053), obtained from the Iranian Research Organization for Science and Technology (IROST). They were incubated overnight on a Sabouraud dextrose agar (Merck KGaA, Darmstadt, Germany) containing chloramphenicol (5 %).

2.8.1. Minimum inhibitory concentration (MIC)

The susceptibility of the studied fungal strains against the *L. royleana* leaf extract and the synthesized AgNPs was assessed by using the broth micro-dilution method as described by Sharifi-Rad et al. [4]. The concentration of the plant extract in the solutions and the phytosynthesized AgNPs in the suspensions ranged from 300 and 2.35 μg mL^{-1}. The primary concentration of the fungi suspension in the RPMI 1640 medium (Sigma, St. Louis, MO, USA) was adjusted to 2.5×10^3 cells mL^{-1}. The wells with the fungi inoculum without the *L. royleana* leaf extract and the synthesized AgNPs were considered as the negative controls. The solutions of fluconazole (as a standard drug used at the same concentration as the plant extract and the synthesized AgNPs) were added to the fungi inoculum, and intended as the positive controls. The microplate-96 plates were incubated for 24 h at 35 °C. After that, the turbidity was observed and its rate was evaluated by the optical density measurements of the content of wells *via* a microplate reader (BioTek, Winooski, VT, USA) at 405 nm.

2.8.2. Minimum fungicidal concentration (MFC)

The minimum fungicidal concentrations (MFC) were evaluated according to the method described by Sharifi-Rad et al. [24]. Briefly, 50 μL from each well of the broth micro-dilution test that showed no observable fungal growth was taken and spread on the Sabouraud dextrose agar (SDA) plates and incubated for 24 h at 35 °C. The lowest concentration that showed no visible fungal growth after the incubation time was considered as the MBC.

2.9. Anti-inflammatory assay

The human red blood cell (RBC) membrane stabilization assay was applied to investigate the anti-inflammatory activity of the *L. royleana* leaf extract and the synthesized AgNPs at different concentrations (25, 50, 100, 150, 200, and 250 μg mL^{-1}) as described by Vane and Botting [32]. The blood samples were obtained from 10 volunteers. Accordingly, an equivalent volume of a sterilized Alsever's solution, containing 0.5 % citric acid, 0.8 % sodium citrate, 0.42 % sodium chloride, and 2 % dextrose, was added to these samples. Then the blood samples were centrifuged at 4000 rpm for 15 min to separate the packed cells. Finally, the cell suspension (10 % v/v) was made in isosaline after the packed cells were cleaned with 0.85 % isosaline (pH 7.2). This human RBC suspension was used to test the anti-inflammatory properties.

As a result, 1 mL of the solutions of the *L. royleana* leaf extract, the suspensions of the synthesized AgNPs, and the diclofenac sodium solutions (a standard drug), all at concentrations of 25, 50, 100, 150, 200, and 250 μg mL^{-1}, were mixed with 2 mL of hyposaline (0.36 %), 1 mL of a phosphate buffer (0.15 mol/L), and 0.5 mL of the human RBC suspension. MQW (2 mL) was used as the control. The resultant solutions were centrifuged at 4000 rpm for 15 min. after being incubated at 37 °C for 30 min. After removing the supernatants, the hemoglobin content was spectrophotometrically determined at 560 nm. The following equation was used to calculate the protection percentage or the human RBC membrane stability-percentage:

$$Protection(\%) = 100 - \left(absorbance_{sample}/absorbance_{control}\right) \times 100$$

2.10. Anti-arthritic assay

The anti-arthritic activity of the *L. royleana* extract and the synthesized AgNPs was determined using the method of Sakat et al. [33] with minor modifications as reported by Elisha et al. [34]. The reaction mixture consisted of the 100 μL the solutions of the plant extract and the suspensions of the synthesized AgNPs (at final concentrations of 25, 50, 100, 150, 200 and 250 μg mL^{-1}) and 100 μL of a 5 % aqueous solution of bovine serum albumin (BSA); pH was adjusted by adding a small volume of glacial acetic acid. The samples were incubated at 37 °C for 20 min and then heated to 70 °C for 10 min. The mixtures were allowed to cool for 10 min, after which their turbidity was measured at 660 nm. The blank comprised the sample and QMW. QMW was used as the negative control. The positive controls were diclofenac sodium at a concentration of 25–250 μg mL^{-1}. The percentage inhibition was calculated using the formula:

$$\%inhibition = 100 \times \left(absorbance_{control} - absorbancetest_{sample}/absorbance_{control}\right)$$

2.11. Cytotoxicity assay

The human hepatocellular carcinoma (Hep-G2) cell line (ATCC®HB8065.) and human breast (MCF-7) cancer cells were purchased from the American Type Culture Collection (ATCC, Rockville, MD, USA). The cells were grown in the Dulbecco's modified Eagle's medium with L-glutamine (2 %), HEPES (N-2-hydroxyethylpiperazine-N-2-ethane sulfonic acid) buffer, heat-inactivated fetal bovine serum (10 %), and 40 g mL^{-1} gentamicin (Sigma-Aldrich, St. Louis, MO, USA).

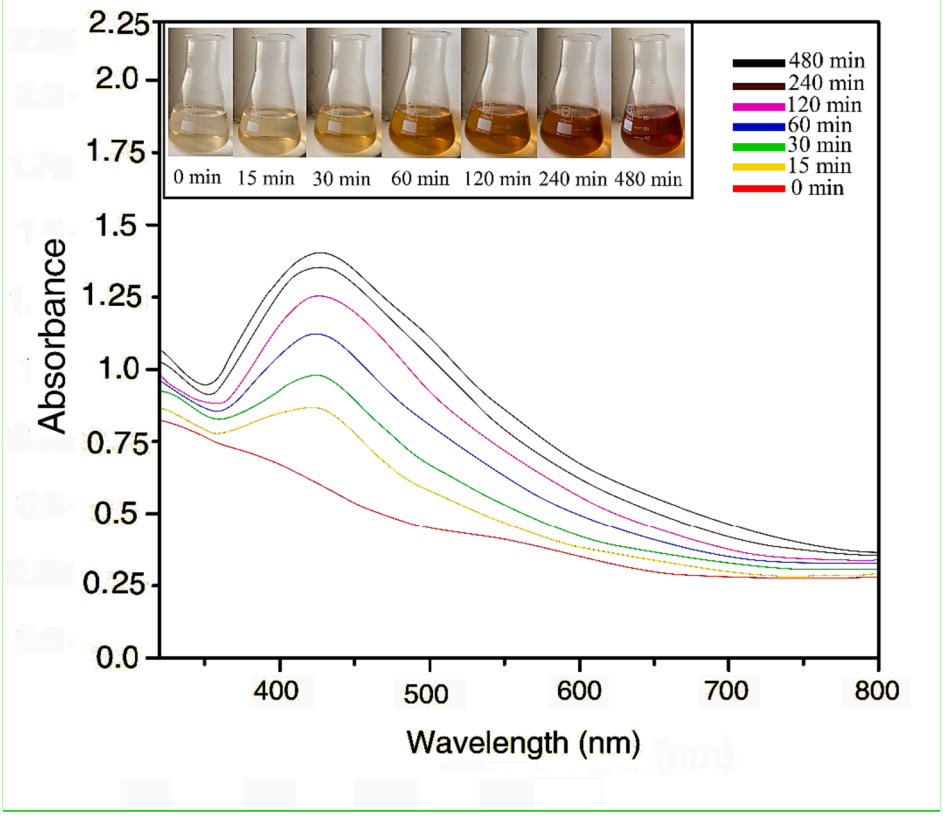

Fig. 1. The UV–Vis absorption spectra of the green-synthesized AgNPs by using the *L. royleana* extract, where the color change of the reaction mixtures due to the formation of AgNPs at different reaction times was noted.

The cells were kept in a humidified atmosphere with CO_2 (5 %) at 37 °C and subcultured four times a week.

The cytotoxic activity of the *L. royleana* extract and the synthesized AgNPs against the cancer cells was examined using the previously described crystal violet staining method reported by Sharifi-Rad et al. [25]. In brief, the cells were incubated in 96-well tissue culture microplates (1 x 10^4 cells per well supplied with 50 µL of a growth media) at 37 °C for 24 h. Then, 50 µL of the solutions of the plant extract or the suspensions of the synthesized AgNPs, both at various concentrations (25, 50, 100, 150, 200 and 250 µg mL^{-1}), were added to each well of the microplates and incubated in a CO_2 incubator at 37 °C for 48 h. 10 µL of a MTT (3-(4,5-dimethylthiazol-2-yl)-2,5-diphenyltetrazolium bromide) (Sigma-Aldrich, St. Louis, MO, USA) stock solution (5 mg mL^{-1} in phosphate buffered saline (PBS, Sigma-Aldrich, St. Louis, MO, USA)) was added to each well and the plates were incubated at 37 °C for 4 h. Then, 100 µL of dimethyl sulfoxide (DMSO) (Merck, Darmstadt, Germany) was added to each well to dissolve the formazan crystals. The absorbance was measured at 595 nm using an automated microplate reader (Beckman Coulter DTX 880 Microplate Reader). Vinblastine sulfate was regarded as a typical anticancer medication and its solutions at concentrations of 25, 50, 100, 150, 200 and 250 µg mL^{-1} were used.

2.12. Catalytic activity of AgNPs

The catalytic efficiency of the synthesized AgNPs was studied in reference to the degradation of methylene blue (MB), following the method reported by Narasaiah et al. [35]. In summary, 150 mL of a sodium borotetrahydrate ($NaBH_4$) solution (10 mmol/L) and 50 mg of the dried AgNPs were mixed thoroughly with 50 mL of a MB solution (2.5×10^{-5} mol/L). 2 mL of the resulting suspensions were taken from the reaction mixtures at different time intervals (0, 2.5, 5, 7.5, and 10 min) and the degradation of MB was monitored using UV–Vis spectrophotometry in the range of 200–800 nm. The degradation rate of MB was measured by UV–Vis spectrophotometer at 664 nm. The catalytic efficiency of the synthesized AgNPs was calculated using the formula:

$$Degradation(\%) = 100 \times (A_0 - A)/A_0$$

where, A_0 is the initial absorbance of MB while A is the absorbance of MB after the degradation.

2.13. Statistical analysis

The statistical analysis was carried out using SPSS software (Version 11.5, SPSS Inc., Chicago, IL, USA). The analysis of variance (ANOVA) followed by the Duncan's multiple range test was used at the 95 % significance level ($\alpha = 0.05$). All experiments were carried out in triplicate, the results were expressed as the mean ± SD values.

3. Results and discussion

3.1. Physicochemical characterization of synthesized AgNPs

3.1.1. Uv–vis absorption spectrophotometry

The UV–Vis absorption spectrophotometric analysis was used to follow and investigate the formation of the green-synthesized AgNPs, as reported previously [31,36], considering that the small spherical AgNPs give a surface plasmon resonance (SPR) band extended in the range from 350 to 500 nm. The optical response of the green-synthesized AgNPs due to their intense SPR band in the spectral region mentioned above confirmed the efficient formation of these NPs as previously reported by Wilson [37].

The rate at which the organic compounds present in the *L. royleana* extract reduced the Ag(I) ions into AgNPs was monitored at different

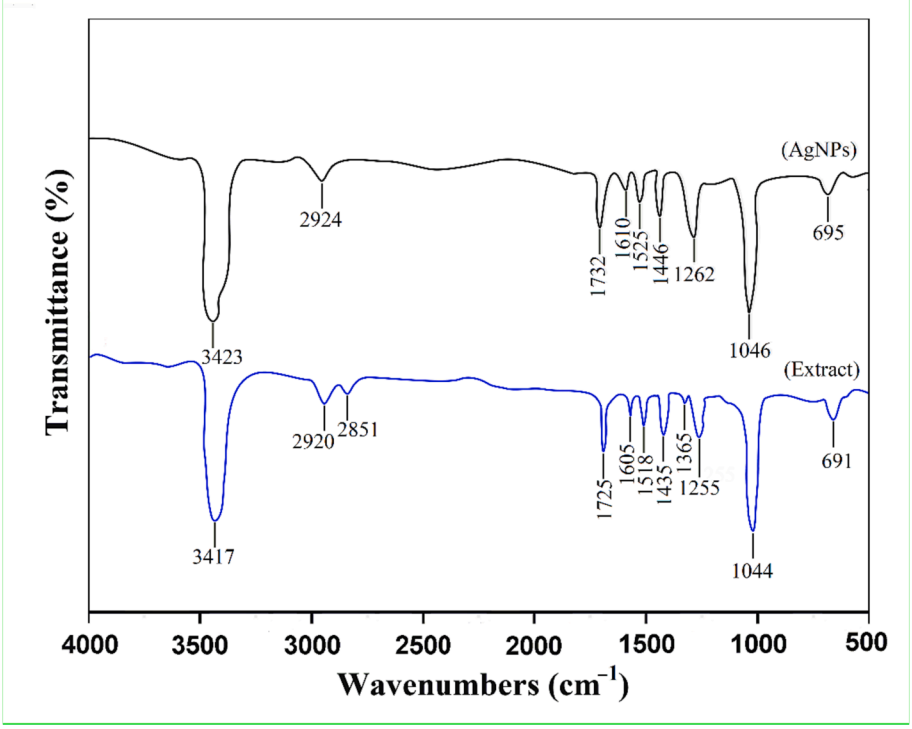

Fig. 2. The Fourier-transform infrared (FT-IR) spectrum of the *L. royleana* extract (blue line) and the green-synthesized AgNPs (black line) (separated from the reaction mixture and cleaned with water).

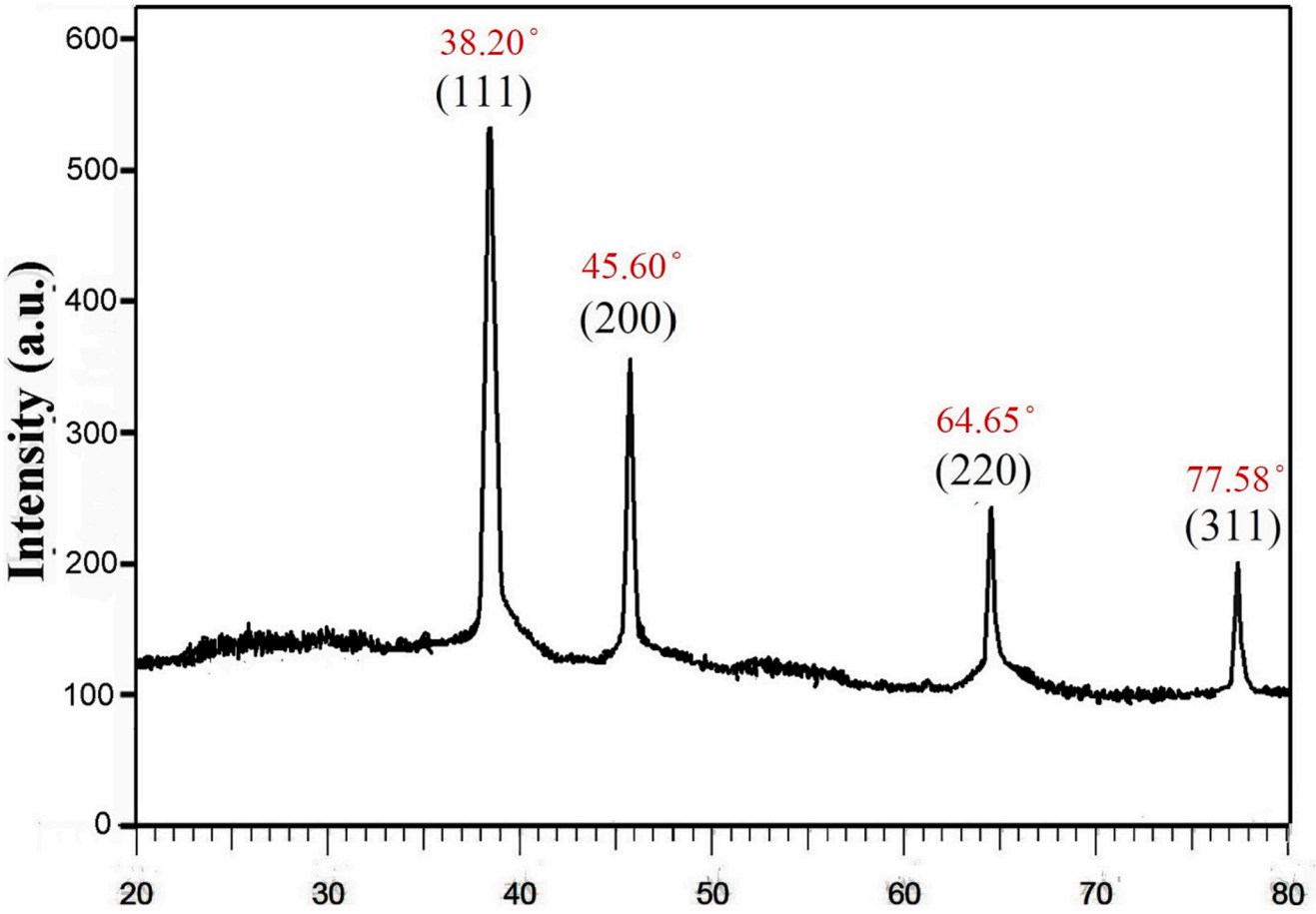

Fig. 3. The X-ray diffraction (XRD) pattern of the green-synthesized AgNPs using the *L. royleana* extract.

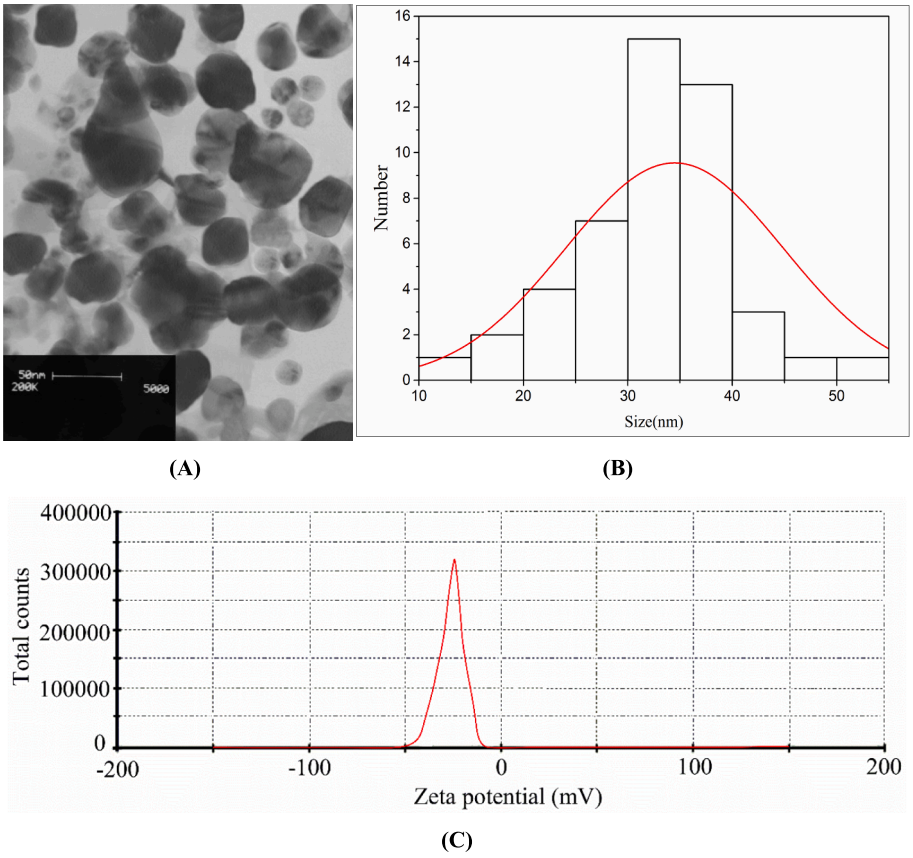

Fig. 4. (**A**) The TEM image, (**B**) the particles size distribution, and **(C)** the zeta potential of the green-synthesized AgNPs using the *L. royleana* extract.

Table 1
The total content of phenolic compounds (TPC), flavonoids (TFC), anthocyanins (TAC), and tannins in the solutions of the *L. royleana* extract and the bio-synthesized AgNPs.

	Concentration (μg mL^{-1})	TPC (mg GAE/g dry weight)	TFC (mg QE/g dry weight)	TAC (mg cyanidin/ 100 g dry weight)	TTC (mg catechin/g dry weight)
Extract	25	24 ± 1^{h}	14 ± 2^{i}	2.3 ± 0.2^{i}	11 ± 1^{h}
	50	38 ± 2^{f}	25 ± 2^{h}	3.4 ± 0.3^{g}	19 ± 2^{f}
	100	57 ± 1^{e}	47 ± 1^{f}	4.8 ± 0.1^{e}	28 ± 2^{d}
	150	89 ± 3^{c}	63 ± 2^{d}	5.7 ± 0.3^{c}	36 ± 3^{c}
	200	104 ± 2^{b}	84 ± 3^{b}	6.8 ± 0.2^{b}	45 ± 1^{b}
	250	125 ± 3^{a}	95 ± 4^{a}	7.6 ± 0.1^{a}	57 ± 2^{a}
AgNPs	25	12 ± 2^{j}	9 ± 2^{j}	1.8 ± 0.2^{j}	7 ± 2^{i}
	50	19 ± 2^{i}	14 ± 3^{i}	2.1 ± 0.1^{ij}	11 ± 1^{h}
	100	34 ± 1^{g}	26 ± 2^{h}	2.9 ± 0.1^{h}	15 ± 3^{g}
	150	58 ± 2^{e}	42 ± 3^{g}	3.4 ± 0.2^{g}	23 ± 2^{e}
	200	76 ± 1^{d}	58 ± 4^{e}	4.2 ± 0.4^{f}	31 ± 1^{d}
	250	91 ± 3^{c}	68 ± 3^{c}	5.3 ± 0.3^{d}	42 ± 3^{b}

Different letters show significant differences among the treatments according to the Duncan's test ($p < 0.05$).

times, i.e., 0, 15, 30, 60, 120, 240, and 480 min. (see Fig. 1). The greatest absorption peak height for the reaction mixtures analysed by UV–Vis absorption spectrophotometry, related to the SPR band of the greenly produced AgNPs, was noted at 425 nm, indicating the formation of spherical NPs. This corroborated quite similar findings reported in other earlier investigations, in which the synthesis of the spherical and/or near-spherical AgNPs was associated with the presence of the maximum of the SPR band in the respective UV–Vis absorption spectra in the range between 410 and 460 nm [4].

Additionally, it was observed that the intensity of the SPR band, which is related to the reaction efficiency, was steadily increased with time. Therefore, the maximal efficiency of the synthesized AgNPs was expected to be obtained after 480 min, where the AgNPs precursor solution ($AgNO_3$) and the leaf extract were mixed. The UV–Vis spectra of the resulting reaction mixtures were also acquired at intervals longer than 480 min and it was established that these spectra were overlapped with the spectra achieved at 480 min that revealed that the reaction was finished.

3.1.2. FT-IR spectroscopy

In order to identify the possible organic biomolecules of the *L. royleana* leaf extract that were accountable for the synthesis of the spherical AgNPs, the FTIR spectroscopy analysis was conducted (Fig. 2). The following absorption peaks were identified in the FTIR spectrum of the synthesized AgNPs in the range from 500 to 4000 cm^{-1}: 3423, 2924, 1732, 1610, 1525, 1446, 1262, 1046, and 695 cm^{-1}. These absorption peaks were ascribed to the stretching vibrations of the OH functional groups (3423 cm^{-1}) in phenols, flavonoids, and alcohols [38], the C–H stretching vibrations (2924 cm^{-1}) in the aromatic structures [39], the C = O stretching vibrations (1732 cm^{-1}) for free ester groups [40], the stretching vibrations of the (NH) C = O group (1610 cm^{-1}) of amide (I) in proteins [41], the stretching vibrations of the C = O or C = C bonds (1525 cm^{-1}) in carboxylic acids or aromatic components [42], the C–O stretching vibrations (1446 cm^{-1}) in polyphenols and polysaccharide [43], the stretching vibrations of the C–H bonds (1262 cm^{-1}) in the methylene (–CH_2–) groups [44], the C–N stretching vibrations (1046 cm^{-1}) in the aliphatic amine groups [45], and finally the C–H stretching vibrations (695 cm^{-1}) of the aromatic components [46]. The FTIR spectrum of the *L. royleana* leaf extract showed the corresponding absorption peaks at 3417, 2920, 1725, 1605, 1518, 1435, 1255, 1044, and 691 cm^{-1}. All the identified absorption peaks in the FTIR spectrum of the AgNPs solution were shifted as compared to those observed in the

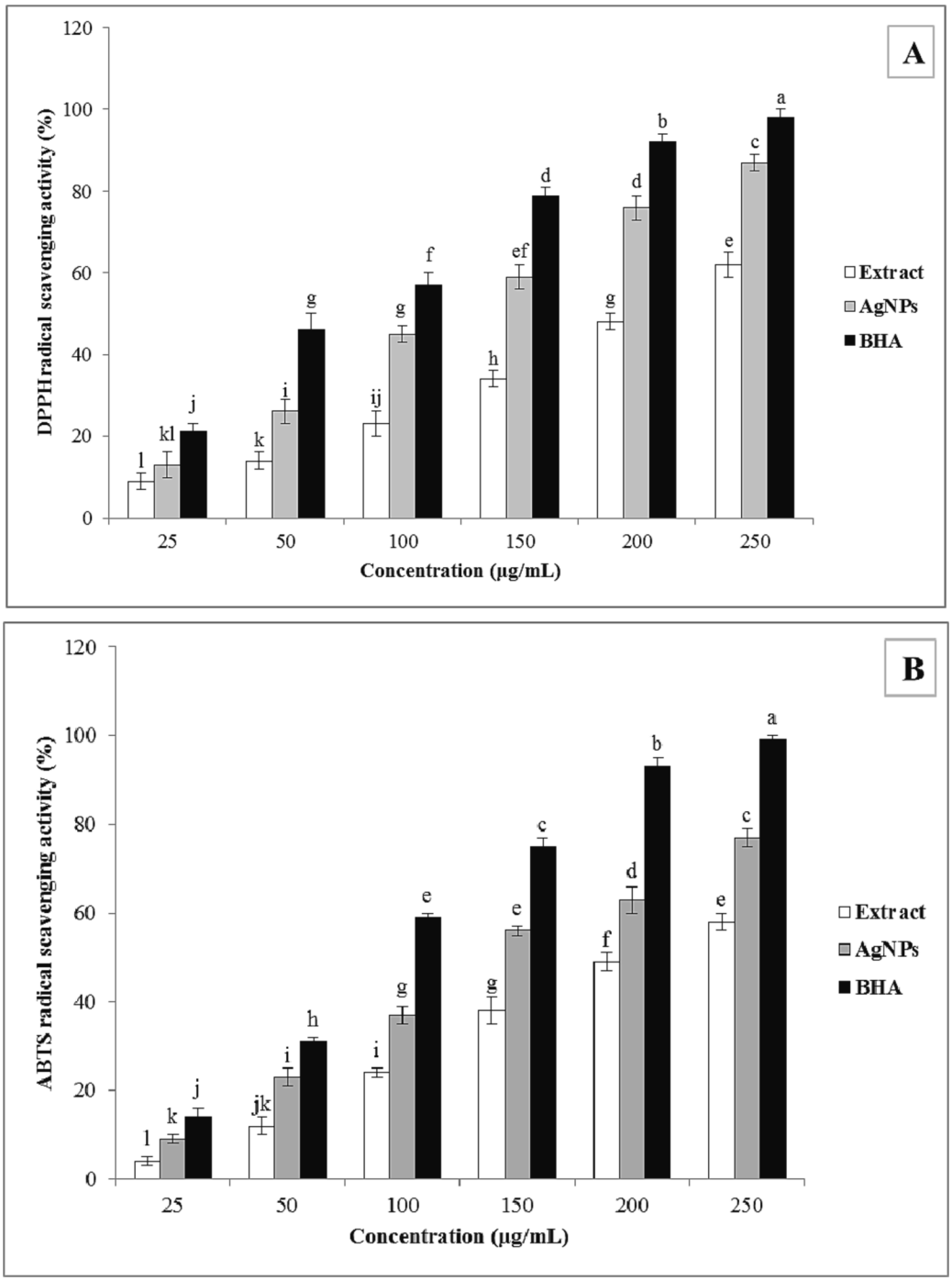

Fig. 5. (**A**) The 2,2-diphenyl-1-picrylhydrazyl (DPPH) radical scavenging activity and (**B**) the 2,2′-azino-bis(3-ethylbenzothiazoline-6-sulfonic acid) (ABTS) radical scavenging activity of the *L. royleana* leaf extract and the green- synthesized AgNPs. Various letters denote significant differences between different tested concentrations based on the Duncan's test ($p < 0.05$).

Table 2
Minimum Inhibitory Concentration (MIC) and Minimum Bactericidal Concentration (MBC) of the *Lallemantia royleana* leaf extract against studied bacterial strains.

	Staphylococcus aureus		*Bacillus cereus*		*Escherichia coli*		*Shigella flexneri*	
	MIC (µg mL^{-1})	MBC (µg mL^{-1})	MIC (µg mL^{-1})	MBC (µg mL^{-1})	MIC (µg mL^{-1})	MBC (µg mL^{-1})	MIC (µg mL^{-1})	MBC (µg mL^{-1})
Extract	75	150	75	150	150	300	150	300
AgNPs	37.5	75	37.5	75	75	150	75	150
Cefalexin	18.75	18.75	18.75	18.75	18.75	18.75	18.75	18.75

Table 3
The antifungal activity of the *L. royleana* leaf extract and the green-synthesized AgNPs.

	Candida glabrata		*Candida albicans*	
	MIC (μg mL^{-1})	MFC (μg mL^{-1})	MIC (μg mL^{-1})	MFC (μg mL^{-1})
Extract	150	300	75	150
AgNPs	75	150	37.5	75
Fluconazole	37.5	37.5	37.5	37.5

The studied MIC concentration: 300–2.34 (μg/mL) (300, 150, 75, 37.5, 18.75, 9.37, 4.68, 2.34).

spectrum of the *L. royleana* leaf extract. This approved that the functional groups of the compounds present in the *L. royleana* leaf extract were involved in the reduction of the Ag (I) ions, being responsible for the synthesis of AgNPs. They also capped the resultant AgNPs, making them stabile in time, biocompatible, and biologically active [23].

3.1.3. X-ray diffraction

The XRD analysis was used to investigate the crystalline structure of the AgNPs synthesized by the *L. royleana* leaf extract (Fig. 3). The distinct diffraction peaks identified at 2θ were 38.20°, 45.60°, 64.65°, and 77.58°; they were indexed to the (111), (200), (220), and (311) planes, respectively, and approved the face-cantered cubic structure of the biosynthesized AgNPs based on the database of Joint Committee on Powder Diffraction Standards (JCPDS), file number 31–1238. The sharpening of the diffraction peaks clearly showed that the resulting Ag crystalline particles were in the nanoparticle regime [47]. Based on the Debye–Sherrer formula, the average crystalline size of the produced AgNPs was assessed as 34.5 nm.

3.1.4. TEM examination, particles size distribution and zeta potential

The TEM analysis (Fig. 4A) clearly approved that the AgNPs synthesized using the *L. royleana* leaf extract were predominantly spherical with some mixed shapes whereas the particle size measured for 50 AgNPs ranged from 13.5 to 69.7 nm with the average of 34.5 ± 1.6 nm (Fig. 4B). In addition, the zeta potential value, being a criterion of the stability of the produced AgNPs, was measured and it was − 24.1 mV (Fig. 4C). This negative value proved the stability of the synthesized AgNPs and this that they were prevented from the agglomeration with time [48]. The negative surface charge of the phytosynthesized AgNPs might be related to the capping action of the biomolecules present in the *L. royleana* leaf extract.

3.2. Phytochemical screening

3.2.1. Total phenolic and flavonoids content

Plants are recognized to serve as a significant source of bioactive substances, such as phenolics, terpenoids, alkaloids, tannins, and anthocyanin [49]. It is established that the aforementioned phytochemicals have a major role in the antioxidant activity of therapeutic plant products. Table 1 displays the results on the TPC and the TFC in the *L. royleana* extract and the green-synthesized AgNPs. In particular, both the leaf extract and the AgNPs enhanced the values of the TPC and the TFC in a dose-dependent manner. The TPC of the *L. royleana* leaf extract and the green-synthesized AgNPs ranged from 24 to 125 mg GAE/ g dry weight and from 12 to 91 mg GAE/ g dry weight, respectively. The leaves extract showed also higher values of the TFC, ranging from 14 to 95 mg QE/ g dry weight, than these for the AgNPs, being in the range from 9 to 68 mg QE/ g dry weight. These findings supported the hypothesis that the phenolic compounds that reduced the Ag(I) ions and stabilized the resulting AgNPs also possibly regulated their functionality and biological activity as reported by Mohanta et al. [50].

3.2.2. Total anthocyanins content

Table 1 also gives the results on the TAC. In particular, the highest TAC (7.0 mg cyanidin/100 g dry weight) was observed in the leaf extract at the highest concentration of 250 μg mL^{-1}, whereas the lowest value

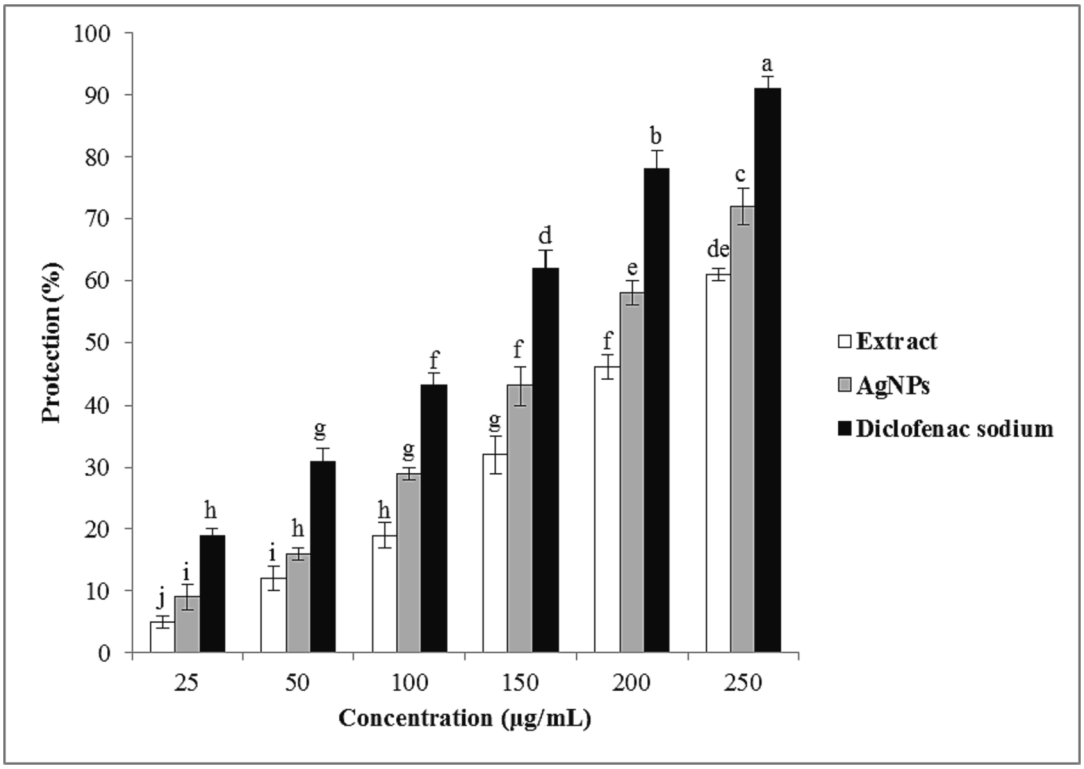

Fig. 6. The anti-inflammatory activity of the *L. royleana* leaf extract and the green-synthesized AgNPs. Various letters denote significant differences between different tested concentrations based on the Duncan's test ($p < 0.05$).

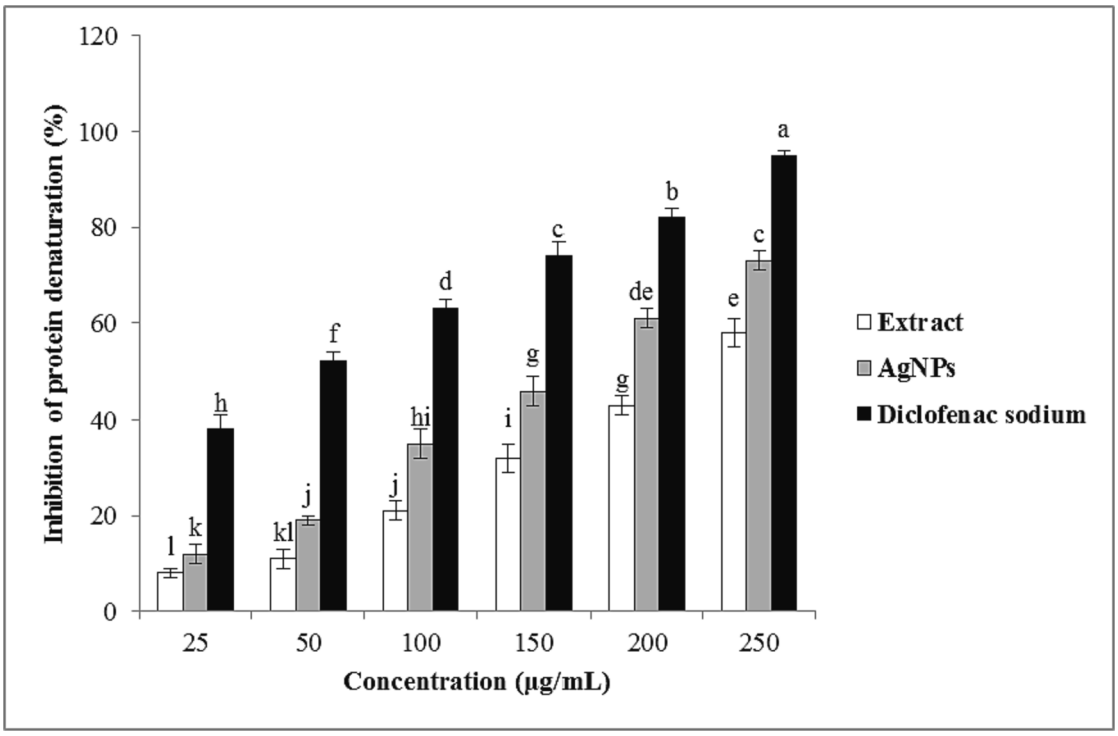

Fig. 7. The anti-arthritic activity of the *L. royleana* leaf extract and the green-synthesized AgNPs. Various letters denote significant differences between different tested concentrations based on the Duncan's test ($p < 0.05$).

(1.8 mg cyanidin/100 g dry weight) was established in the case of the green-synthesized AgNPs at the lowest concentration of 25 µg mL^{-1}.

3.2.3. Total tannins concentration

The results on the TTC are included in Table 1 as well. The maximum TTC (57.0 mg catechin/g dry weight) was measured for the leaf extract of *L. royleana* whereas the lowest value (7.0 mg catechin/g dry weight) was noted in the case of the green-synthesized AgNPs.

According to the results, the synthesized AgNPs had lower phytochemical compounds as compared to the *L. royleana* leaf extract. These results confirmed that not all metabolites and antioxidant compounds are applied to reduce the Ag(I) ions, but they also act as the capping agents [51]. Similar to these results, Labulo et al. [52] reported that the green synthesized AgNPs by the *Morinda lucida* leaf extract had a lower content of the phytochemical compounds.

3.3. Antioxidant assay

3.3.1. DPPH assay

Using the DPPH reagent, the antioxidant capacity of the leaf extract and AgNPs, as reported by Baliyan et al. [53], was evaluated (see Fig. 5A). The antiradical activity of the positive control (BHA) was followed by this assessed for the biosynthesized AgNPs, whereas the leaf extract showed the lowest value of the DPPH radical scavenging activity. Additionally, it was noted that the leaf extract and the synthesized AgNPs steadily enhanced their capacity to scavenge the free DPPH radicals as their concentrations were increased up to 250 µg mL^{-1}. Particularly, the AgNPs demonstrated the strongest antioxidant activity, being 87 % at the maximum prepared concentration of 250 µg mL^{-1}. At the same tested concentration, the antioxidant activity of the leaf extract was by about 25 % lower.

3.3.2. ABTS assay

The ABTS method is often applied to measure the antioxidant properties of the H-atoms-donating and chain-breaking antioxidants in phytomedicine studies [54]. Generally, the obtained results showed that the antioxidant activity of the synthesized AgNPs was lower than this assessed for the positive control (BHA) (Fig. 5B). Particularly, the AgNPs demonstrated the strongest antioxidant activity, being 77 % at the maximum analyzed concentration of 250 µg mL^{-1}. Concurrently, the antioxidant activity determined for the leaf extract at the same concentration was only 58 %. The results, obtained using the both methods, clearly indicated that the scavenging activity of the biosynthesized AgNPs are attributed to both the phytochemicals coating their surface and elemental Ag, as reported by Macovei et al. [55].

3.4. Antibacterial assays

3.4.1. Minimum inhibitory concentration (MIC) and minimum bactericidal concentration (MBC)

The results of the MIC and the MBC values for the *L. royleana* leaf extract and the synthesized AgNPs are presented in Table 2. Based on them, it is evident that the phytosynthesized AgNPs were more biologically active toward the studied bacteria strains as compared to the *L. royleana* leaf extract. The MIC values for the synthesized AgNPs against the tested bacteria strains were varied from 37.5 to 75 µg mL^{-1} whereas these values for the *L. royleana* leaf extract ranged from 75 to 150 µg mL^{-1}. The MBC values for the synthesized AgNPs and the *L. royleana* leaf extract ranged from 75 to 150 µg mL^{-1} and 150 to 300 µg mL^{-1}, respectively.

3.5. Antifungal activity

3.5.1. Minimum fungicidal concentration (MFC)

Table 3 illustrates the antifungal activity of *L. royleana* leaf extract and the green-synthesized AgNPs. The antifungal activity, expressed as the MIC, of the AgNPs against all studied fungi changed from 37.5 to 75.0 µg mL^{-1}, and was higher than this of the *L. royleana* leaf extract with the MIC values varying from 75.0 to 150 µg mL^{-1} against *C. albicans* and *C. glabrata*, respectively. This difference was also noted in the case of the MFC values assessed for the produced AgNPs and the *L. royleana* leaf extract; they changed from 75.0 to 150 and from 150 to

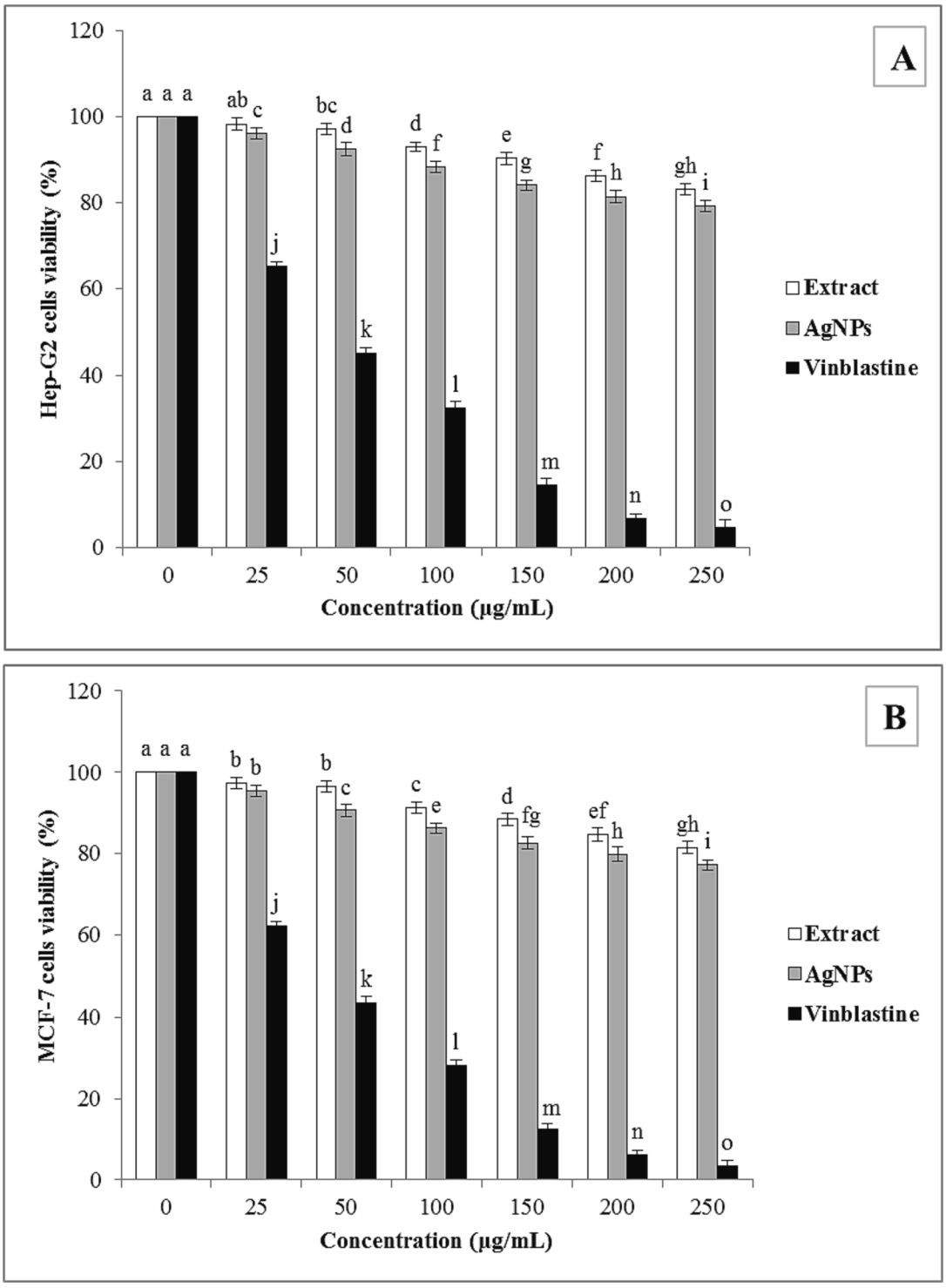

Fig. 8. The cytotoxic activity of the *L. royleana* leaf extract and the green-synthezed AgNPs against Hep-G2 and MCF-7 cell lines. Various letters denote significant differences between different tested concentrations based on the Duncan's test ($p < 0.05$).

300 µg mL^{-1}, respectively.

3.5.1.1. Mechanisms of antimicrobial activity. The beneficial biocidal characteristics of the AgNPs was likely attributable to their shape, size, and the surface coating, as suggested before by other researchers [56,57,58]. Most notably, the AgNPs have a large contact area with the microorganisms due to their smaller size and higher surface to volume proportions. This features of AgNPs greatly improve their biological and chemical characteristics, making them a potent bactericidal substance. The AgNPs are also capable of stopping biological processes such the respiration and the cell permeability. Additionally, the AgNPs have the ability to disturb the biological components when they enter the cell membranes by reacting with P- and S-mediated complexes such deoxyribonucleic acid (DNA) complexes [59,60]. This widespread disruption of the cell structure and its function certainly decreased their resistance to the antifungal effect of the synthesized AgNPs.

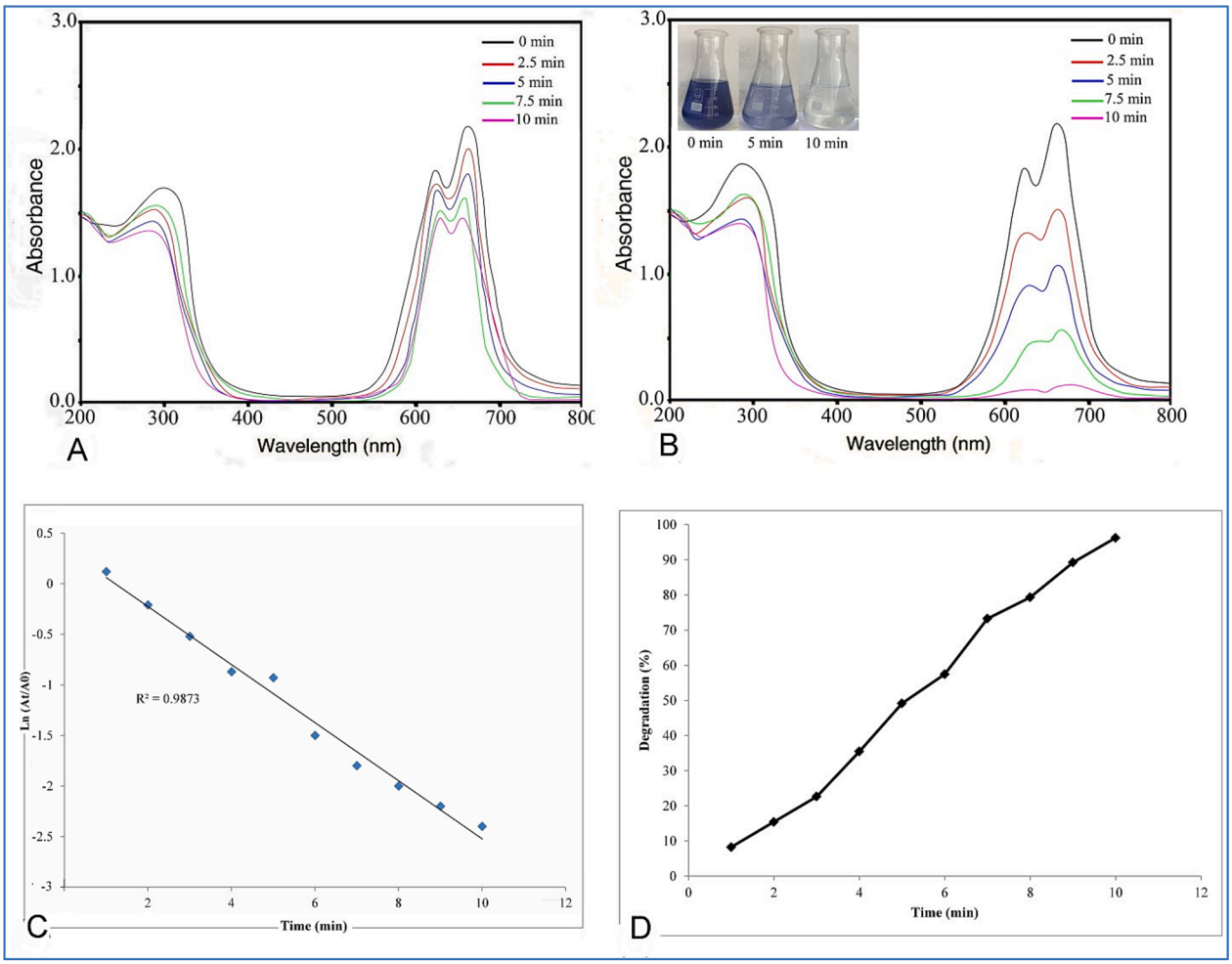

Fig. 9. The catalytic activity of the phytosynthesized AgNPs in reference to the degradation of methylene blue (MB) dye (A) reaction mixture without the AgNPs (B) reaction mixture with the AgNPs (C) the kinetics of the catalytic activity of the AgNPs, and (D) the % MB degradation of the AgNPs.

3.6. Anti-inflammatory assay

Using the human RBC membrane stabilization assay, the examination of the anti-inflammatory activity of the *L. royleana* leaf extract and the green-synthesised AgNPs was carried out. According to the findings given in Fig. 6, the biosynthesized AgNPs were established to have a higher stabilizing capability on the human RBC membrane than the *L. royleana* leaf extract did. The green-synthesized AgNPs were found to have a concentration-dependent membrane stabilizing ability that was ranged from 9 to 72 %. Although the AgNPs were lately reported to play a significant role in combating the inflammation, some investigations found that their anti-inflammatory effects are still very modest [61,62]. Recently, Khashan et al. [63] suggested that the application of AgNPs showed the stronger anti-inflammatory effect than dexamethasone.

3.7. Anti-arthritic assay

The anti-denaturation study with BSA was performed to investigate the anti-arthritis activity of the *L. royleana* leaf extract and the green-synthesized AgNPs. When BSA is heated, it undergoes denaturation and antigens are expressed that are associated with the type-III hypersensitivity reaction, which in turn is related to such diseases as serum sickness, glomerulonephritis, rheumatoid arthritis and systemic lupus erythematosus [64].

The studied *L. royleana* leaf extract and the green-synthesized AgNPs showed *in vitro* anti-arthritic activity in a dose dependent manner higher than the positive control, i.e., diclofenac sodium. The inhibition of the protein denaturation (%) of the leaf extract and the AgNPs ranged from 8 and 58 % and from 12 to 73 %, respectively (Fig. 7). These results were very promising because indicated the possible use of the applied plant extract and the biosynthesized AgNPs as an alternative for the arthritis, rheumatism and other inflammatory conditions, as was mentioned also in [65,66].

3.8. Cytotoxicity assay

The cytotoxicity activity results are illustrated in Fig. 8 (A,B). In particular, the *L. royleana* leaf extract and the green-synthesized AgNPs exhibited the cytotoxic effect against the two tested cancer cell lines in a dose-dependent manner. Generally, both the leaf extract and the prepared AgNPs demonstrated a significantly higher activity than the positive control, being vinblastine sulphate at the same studied concentrations. Mundekkad and Cho [67] reported that the reactive oxygen species (ROS)-mediated apoptosis is the most crucial process through which NPs generally cause the apoptosis in the cancer cells. Other ways that the NPs work to induce the apoptosis in the cancer cells are the up- and down-regulation of proteins, the immunological interventions, the transcription inhibition, the site-specific cytotoxicity, etc. There is no doubt that the natural compounds have attracted the scientific community's attention in the hunt for more effective and less toxic medications for the treatment of different kinds of cancer diseases [68,69]. Many natural compounds extracted from herbs, such as *Nepeta juncea* Benth. [25], *Origanum vulgare* [70], *Tetraclinis articulata* [71], were lately demonstrated to have a promising anti-cancer activity

against human breast adenocarcinoma (MCF-7), human hepatocellular (Hep-G2) and lung cancer cells (A549), respectively.

3.9. Catalytic activity of AgNPs

The catalytic activity of the phytosynthesized AgNPs in the presence of $NaBH_4$ was evaluated using the UV–Vis absorption spectroscopy (Fig. 9A). According to the results, after the addition of the phytosynthesized AgNPs to the mixture, the catalytic reduction of MB occurred and the color of the mixture was changed from blue to completely colorless. The absorbance of the respective absorption band of MB (at 664 nm) gradually decreased over the time that confirmed the biocatalytic activity of the phytosynthesized AgNPs in this degradation reaction (Fig. 9B). Furthermore, according to the degradation percentage of MB, this dye was degraded within 10 min of incubation (Fig. 9C).

The previous studies also proved that the green synthesized AgNPs had the significant catalytic activity [72]. During the chemical reaction, the bond dissociation energy had a significant role in the formation of new bonds and/or the bands breaking. During the reaction between the MB dye and $NaBH_4$, the electron transfer took place, where $NaBH_4$ acted as a donor and the MB dye as an acceptor [73]. The addition of the Ag nanocatalyst to the reaction mixture acted as a potential mediator between the MB dye and the BH_4 ions. First, it led to a decrease in the bond dissociation energy and made the electron transfer between them more efficient. Therefore, the amount of the MB dye reduction by $NaBH_4$ increased significantly in the presence of the applied AgNPs [74].

4. Conclusion

A rapid, plant-mediated, and green method of the synthesis of AgNPs was successfully carried out by using the *L. royleana* leaf extract. It was found that various biomolecules of the *L. royleana* leaf extract were responsible for the production of the AgNPs and their stability. The SPR absorption band at 425 nm and the XRD pattern approved the AgNPs formation. The resulting AgNPs were predominantly spherical with some mixed shapes and crystalline with the average size of 34. 5 ± 1.6 nm according to the TEM analysis. The FTIR spectroscopy confirmed that the capping of the produced AgNPs with the phytocompounds originating from the extract occurred. The zeta potential value was −24.1 mV, indicating the stability of produced AgNPs. The phytosynthesized AgNPs showed potent antioxidant, antimicrobial, anti-inflammatory, anti-arthritic and cytotoxic activities, proving in this way that they can be considered for the development of new drugs. The catalytic activity of the phytosynthesized AgNPs was also indicated when applied them for the MB degradation in the presence of $NaBH_4$. Summering, the current study provides a promising way of the green synthesis of AgNPs by the *L. royleana* leaf extract with the very significant biopharmaceutical and catalytic applications.

CRediT authorship contribution statement

Majid Sharifi-Rad: Writing – review & editing, Writing – original draft, Visualization, Validation, Supervision, Software, Resources, Project administration, Methodology, Investigation, Funding acquisition, Formal analysis, Data curation, Conceptualization. **Hazem S. Elshafie:** Writing – original draft. **Pawel Pohl:** Writing – review & editing, Writing – original draft.

Declaration of Competing Interest

The authors declare that they have no known competing financial interests or personal relationships that could have appeared to influence the work reported in this paper.

Data availability

No data was used for the research described in the article.

Acknowledgment

This research was funded by the University of Zabol, Zabol, Iran (grant number: IR-UOZ-GR-9186).

References

[1] Z. Zhang, H. Karimi-Maleh, In situ synthesis of label-free electrochemical aptasensor-based sandwich-like AuNPs/PPy/Ti3C2Tx for ultrasensitive detection of lead ions as hazardous pollutants in environmental fluids, Chemosphere 324 (2023), 138302.
[2] H. Karimi-Maleh, M. Ghalkhani, Z.S. Dehkordi, J. Singh, Y. Wen, M. Baghayeri, J. Rouhi, L. Fu, S. Rajendran, MOF-enabled pesticides as developing approach for sustainable agriculture and reducing environmental hazards, J. Ind. Eng Chem (2023).
[3] H. Zhang, Karimi-Maleh, Label-free electrochemical aptasensor based on gold nanoparticles/titanium carbide MXene for lead detection with its reduction peak as index signal, Adv. Compos. Hybrid Mater. 6 (2023) 68.
[4] M. Sharifi-Rad, P. Pohl, F. Epifano, Phytofabrication of Silver Nanoparticles (AgNPs) with pharmaceutical capabilities using Otostegia persica (Burm.) Boiss. leaf extract, Nanomaterials 11 (2021) 1045.
[5] Y. Karimi-Maleh, Z. Liu, R. Li, Y. Darabi, C. Orooji, F. Karaman, M. Karimi, J. Baghayeri, L. Rouhi, S. Fu, Rostamnia, Calf thymus ds-DNA intercalation with pendimethalin herbicide at the surface of ZIF-8/Co/rGO/C3N4/ds-DNA/SPCE A Bio-Sensing Approach for Pendimethalin Quantification Confirmed by Molecular Docking Study, Chemosphere. 332 (2023), 138815.
[6] S. Abd-Ellatif, A. A. Ibrahim, F.A. Safhi, E. S. Abdel Razik, S. S. A. Kabeil, S. Aloufi, A. A. Alyamani, M. M. Basuoni, S. M. ALshamrani, H. S. Elshafie, Green synthesized of *Thymus vulgaris* chitosan nanoparticles induce relative WRKY-genes expression in *Solanum lycopersicum* against *Fusarium solani*, the Causal Agent of Root Rot Disease, Plants. 11 (2022) 3129.
[7] N.K. Gour, Jain, Advances in green synthesis of nanoparticles, Artif, Cells Nanomed, Biotechnol. 47 (2019) 844–851.
[8] I.I. Buzea, K.R. Pacheco, Nanomaterials and nanoparticles: sources and toxicity, Biointerphases 2 (2007) MR17-MR71.
[9] S. Behboodi, F. Baghbani-Arani, S. Abdalan, S.A. Sadat Shandiz, Green engineered biomolecule-capped silver nanoparticles fabricated from Cichorium intybus extract: in vitro assessment on apoptosis properties toward human breast cancer (MCF-7) cells, Biol. Trace Elem. Res. 187 (2019) 392–402.
[10] M. Jeyaraj, M. Rajesh, R. Arun, D. MubarakAli, G. Sathishkumar, G. Sivanandhan, G. Kapil Dev, M. Manickavasagam, K. Premkumar, N. Thajuddin, A. Ganapathi, An investigation on the cytotoxicity and caspase-mediated apoptotic effect of biologically synthesized silver nanoparticles using *Podophyllum hexandrum* on human cervical carcinoma cells, Colloids and Surf. b: Biointerfaces. 102 (2013) 708–717.
[11] F. Okafor, A. Janen, T. Kukhtareva, V. Edwards, M. Curley, Green synthesis of silver nanoparticles, their characterization, application and antibacterial activity, Int. J. Environ. Res. Public Health. 10 (2013) 5221–5238.
[12] M. Dhayalan, P. Karikalan, M. R. S. Umar, N. Srinivasan, Biomedical applications of silver nanoparticles. in silver micro-nanoparticles-properties, synthesis, characterization, and applications, IntechOpen. 2021.
[13] U. Manik, A. Nande, S. Raut, S. Dhoble, Green synthesis of silver nanoparticles using plant leaf extraction of *Artocarpus heterophylus* and *Azadirachta indica*, Res. Mater. 6 (2020), 100086.
[14] R. Gengan, K. Anand, A. Phulukdaree, A. Chuturgoon, A549 lung cell line activity of biosynthesized silver nanoparticles using *Albizia adianthifolia* leaf, Colloids Surf. b: Biointerfaces. 105 (2013) 87–91.
[15] P.R. Meena, A.P. Singh, K.K. Tejavath, Biosynthesis of silver nanoparticles using *Cucumis prophetarum* aqueous leaf extract and their antibacterial and antiproliferative activity against cancer cell lines, ACS Omega 5 (2020) 5520.
[16] M.S. Verma, Mehata, Controllable synthesis of silver nanoparticles using neem leaves and their antimicrobial activity, J. Radiation Res. Applied Sci. 9 (2016) 109–115.
[17] G. Marslin, K. Siram, Q. Maqbool, R.K. Selvakesavan, D. Kruszka, P. Kachlicki, G. Franklin, Secondary metabolites in the green synthesis of metallic nanoparticles, Materials 11 (2018) 940.
[18] T.M. Moghaddam, S.M.A. Razavi, B. Emadzadeh, Rheological interactions between *Lallemantia royleana* seed extract and selected food hydrocolloids, J. Sci. Food Agric. 91 (2010) 1083–1088.
[19] F. Naghibi, M. Mosaddegh, M. Mohammadi Motamed, A. Ghorbani, Labiatae Family in folk Medicine in Iran: from Ethnobotany to Pharmacology, Iran. J. Pharm. Res. 4 (2005) 63–79.
[20] S.M.A. Razavi, T.M. Moghaddam, A.M. Amini, Physicomechanic and chemical properties of Balangu seed, Int. J. Food Eng. 4 (2008) 1–12.
[21] M. Bahramparvar, M.H. Haddad Khodaparast, S.M.A. Razavi, The effect of Lallemantia royleana (Balangu) seed, palmate-tuber salep and carboxymethylcellulose gums on the physicochemical and sensory properties of typical soft ice cream, Int. J. Dairy Technol. 62 (2009) 571–576.

[22] M. Amini, Extraction optimization of Balangu seed gum and effect of Balangu seed gum on the rheological and sensory properties of Iranian flat bread, Ferdowsi University of Mashhad, Iran, 2007. MSc thesis.

[23] M. Sharifi-Rad, P. Pohl, F. Epifano, J.M. Álvarez-Suarez, Green synthesis of silver nanoparticles using *Astragalus tribuloides* delile. root extract: Characterization, antioxidant, antibacterial, and anti-inflammatory activities, Nanomaterials 10 (2020) 238.

[24] M. Sharifi-Rad, P. Pohl, Synthesis of biogenic silver nanoparticles (Agcl-NPs) using a Pulicaria vulgaris Gaertn. aerial part extract and their application as antibacterial, antifungal and antioxidant agents, Nanomaterials 10 (2020) 638.

[25] M. Sharifi-Rad, F. Epifano, S. Fiorito, J.M. Álvarez-Suarez, Phytochemical analysis and biological investigation of Nepeta juncea Benth, Different Extracts, Plants. 9 (2020) 646.

[26] X. Dewanto, K. Wu, K. Adom, R.H. Liu, Thermal processing enhances the nutritional value of tomatoes by increasing total antioxidant activity, J. Agric. Food Chem. 50 (2002) 3010–3014.

[27] C.C. Chang, M.H. Yang, H.M. Wen, J.C. Chern, Estimation of total flavonoid content in propolis by two complementary colorimetric methods, J. Food Drug Anal. 10 (2002) 178–182.

[28] D.J. Vega-arroy, H. Ruíz-espinosa, J.J. Luna-guevara, M.L. Luna-guevara, P. Hernández-carranza, R. Ávila-sosa, C.E. Ochoa-velasco, Effect of solvents and extraction methods on total anthocyanins, phenolic compounds and antioxidant capacity of Renealmia alpinia (Rottb.) Maas peel, Czech J. Food Sci. 35 (2017) 456–465.

[29] B. Sun, J.M. Richardo-Da-Silvia, I. Spranger, Critical factors of vanillin assay for catechins and proanthocyanidins, J. Agric. Food Chem. 46 (1998) 4267–4274.

[30] K. Min-Jung, N. Hwa-Hyun, C. Myong-Soo, Subcritical water extraction of bioactive compounds from Orostachys japonicus A. Berger (Crassulaceae), Sci. Rep. 10 (2020) 10890.

[31] Clinical and Laboratory Standards Institute (CLSI), Reference Method for dilution antimicrobial susceptibility tests for bacteria that grow aerobically; approved standard M7-A6; National Committee for Clinical Laboratory Standards: Wayne, PA, USA, 2012.

[32] J. Vane, R. Botting, New insights into the mode of action of anti-inflammatory drugs, Inflamm. Res. 44 (1995) 1–10.

[33] S.S. Sakat, A.R. Juvekar, M.N. Gambhire, In-vitro antioxidant and anti-inflammatory activity of methanol extract of *Oxalis corniculata* Linn, Int. J. Pharm. Pharm Sci. 2 (2010) 146–155.

[34] L. Elisha, J.P. Dzoyem, L.J. McGaw, F.S. Botha, J.N. Eloff, The anti-arthritic, anti-inflammatory, antioxidant activity and relationships with total phenolics and total flavonoids of nine South African plants used traditionally to treat arthritis, BMC Complement. Altern. Med. 16 (2016) 1–10.

[35] P. Narasaiah, B.K. Mandal, S. Nallani Chakravarthula, Synthesis of gold nanoparticles by cotton peels aqueous extract and their catalytic efficiency for the degradation of dyes and antioxidant activity, IET Nanobiotechnol. 12 (2018) 156–165.

[36] T. Tsuji, K. Iryo, N. Watanabe, M. Tsuji, Preparation of silver nanoparticles by laser ablation in solution: influence of laser wavelength on particle size, Appl. Surf. Sci. 85 (2002) 202.

[37] O. Wilson, G.J. Wilson, P. Mulvaney, Laser writing in polarized silver nanorod films, Adv. Mater. 14 (2002) 1000.

[38] A.O. Dada, F.A. Adekola, E.O. Odebunmi, Liquid phase scavenging of Cd (II) and Cu (II) ions onto novel nanoscale zerovalent manganese (nZVMn): Equilibrium, kinetic and thermodynamic studies, Environ. Nanotechnol. Monit. Manag. 8 (2017) 63–72.

[39] A.G. Femi-Adepoju, A.O. Dada, K.O. Otun, A.O. Adepoju, O.P. Fatoba, Green synthesis of silver nanoparticles using terrestrial fern (Gleichenia Pectinata (Willd.) C. Presl.): Characterization and antimicrobial studies, Heliyon. 5 (2019) e01543.

[40] S. Boukir, P. Fellak, Doumenq, Structural characterization of Argania spinosa Moroccan wooden artifacts during natural degradation progress using infrared spectroscopy (ATR-FTIR) and X-Ray diffraction (XRD), Heliyon. 5 (2019).

[41] S. Azizi, F. Namvar, M. Mahdavi, M.B. Ahmad, R. Mohamad, Biosynthesis of silver nanoparticles using brown marine macroalga Sargassum Muticum aqueous extract, Materials. 6 (2013) 5942–5950.

[42] Y. Singh, R. S. Sodhi, P. P. Singh, S. Kaushal, Biosynthesis of NiO nanoparticles using Spirogyra sp. cell-free extract and their potential biological applications, Mater. Adv. 3(2022) 4991-5000.

[43] M. Radwan, E.F. Aboelfetoh, T. Kimura, T.M. Mohamed, M.M. El-Keiy, Fenugreek-mediated synthesis of zinc oxide nanoparticles and evaluation of its in vitro and in vivo antitumor potency, Biomed. Res. Ther. 8 (2021) 4483–4496.

[44] J. Zajac, M. Hanuza, L.D. Wandas, Determination of N-acetylation degree in chitosan using Raman spectroscopy. Spectrochim, Acta Part A Mol, Biomol. Spectrosc. 134 (2015) 114–120.

[45] S.H. Lim, E.Y. Ahn, Y. Park, Green synthesis and catalytic activity of gold nanoparticles synthesized by *Artemisia capillaris* water extract, Nanoscale Res. Lett. 11 (2016) 1–11.

[46] H. Muthukumar, S.K. Palanirajan, M.K. Shanmugam, S.N. Gummadi, Plant extract mediated synthesis enhanced the functional properties of silver ferrite nanoparticles over chemical mediated synthesis, Biotechnol. Rep. 26 (2020) e00469.

[47] J. Ashok, R.K. Bhagyashree, Z. Ameeta, Smita, Banana peel extract mediated synthesis of gold nanoparticles, Colloids Surf. b: Biointerfaces. 80 (2009) 45–50.

[48] S.V. Patil, H.P. Borase, C.D. Patil, B.K. Salunke, Biosynthesis of silver nanoparticles using latex from few euphorbian plants and their antimicrobial potential, Appl. Biochem. Biotechnol. 167 (2012) 776–790.

[49] J. Dai, R.J. Mumper, Plant phenolics: extraction, analysis and their antioxidant and anticancer properties, Molecules 15 (2010) 7313–7352.

[50] Y.K. Mohanta, S.K. Panda, K. Biswas, A. Tamang, J. Bandyopadhyay, D. De, D. Mohanta, A.K. Bastia, Biogenic synthesis of silver nanoparticles from Cassia fistula (Linn.): In vitro assessment of their antioxidant, antimicrobial and cytotoxic activities, IET Nanobiotechnol. 10 (2016) 438–444.

[51] S.S. Shoor, M. Lodise, Rapidsynthesis of Au, Ag, and bimetallic Au coree Ag shell nanoparticles using Neem (*Azadirachta indica*) leaf broth, J. Colloid Interface Sci.275 (20062) 496.

[52] A.H. Labulo, O.A. David, A.D. Terna, Green synthesis and characterization of silver nanoparticles using *Morinda lucida* leaf extract and evaluation of its antioxidant and antimicrobial activity, Chem. Pap. 76 (2022) 7313–7325.

[53] S. Baliyan, R. Mukherjee, A. Priyadarshini, A. Vibhuti, A. Gupta, R.P. Pandey, C. M. Chang, Determination of antioxidants by DPPH radical scavenging activity and quantitative phytochemical analysis of Ficus religiosa, Molecules 27 (2022) 1326.

[54] R. Ilyasov, V.L. Beloborodov, I.A. Selivanova, R.P. Terekhov, ABTS/PP decolorization assay of antioxidant capacity reaction pathways, Int. J. Mol. Sci. 21 (2020) 1131.

[55] Macovei, S. V. Luca, K. Skalicka-Woźniak, C .E. Horhogea, C. M. Rimbu, L. Sacarescu, G. Vochita, D. Gherghel, B. L. Ivanescu, A. D. Panainte, C. Nechita, Silver nanoparticles synthesized from *Abies alba* and *Pinus sylvestris* Bark extracts: characterization, antioxidant, cytotoxic, and antibacterial effects, Antioxidants. 12 (2023) 797.

[56] X.-F. Zhang, Z.-G. Liu, W. Shen, S. Gurunathan, Silver nanoparticles: synthesis, characterization, properties, applications, and therapeutic approaches, Int. J. Mol. Sci. 17 (2016) 1534.

[57] M. Rai, A. Yadav, A. Gade, Silver nanoparticles as a new generation of antimicrobials, Biotechnol. Adv. 27 (2009) 76–83.

[58] S. Kim, E. Kuk, K.N. Yu, J.H. Kim, S.J. Park, H.J. Lee, S.H. Kim, Y.K. Park, Y. H. Park, C. y., Hwang Antimicrobial effects of silver nanoparticles, Nanomed. Nanotechnol. 3 (2007) 95–101.

[59] S. Pal, Y.K. Tak, J.M. Song, Does the antibacterial activity of silver nanoparticles depend on the shape of the nanoparticle? A study of the gram-negative bacterium Escherichia coli, Appl. Environ. Microbiol. 73 (2007) 1712–1720.

[60] O. Choi, K.K. Deng, N.J. Kim, L. Ross, R.Y. Surampalli, Z. Hu, The inhibitory effects of silver nanoparticles, silver ions, and silver chloride colloids on microbial growth, Water Res. 42 (2008) 3066–3074.

[61] K.C. Bhol, P.J. Schechter, Effects of nanocrystalline silver (NPI 32101) in a rat model of ulcerative colitis, Dig. Dis. Sci. 52 (2007) 2732–2742.

[62] J. Tian, K.K. Wong, C.M. Ho, C.N. Lok, W.Y. Yu, C.M. Che, J.F. Chiu, P.K. Tam, Topical delivery of silver nanoparticles promotes wound healing, ChemMedChem Chem. Enabling Drug Discov. 2 (2007) 129–136.

[63] A. Khashan, Y. Dawood, Y.H. Khalaf, Green chemistry and anti-inflammatory activity of silver nanoparticles using an aqueous curcumin extract, Results Chem. 5 (2023), 100913.

[64] G. Kishore, G. Siva, E.S. Sindhu, In Vitro anti-inflammatory and anti-arthritic activity of leaves of *Physalis Angulata* L, Int. J. Pharmacetical Ind. Res. 1 (2011) 211–213.

[65] M. Choudhary, V. Kumar, H. Malhotra, S. Singh, Medicinal plants with potential anti-arthritic activity, J. Intercult. Ethnopharmacol. 4 (2015) 147–179.

[66] Arya, M. Meena, G. Neha, P. Vidya, In vitro anti-inflammatory and antiarthritic activity in methanolic extract of *Cocculus hirsutus* (L.) Diels. In vivo and In vitro, Int. J. Pharm. Sci. Res. 5 (2014) 1957–62.

[67] W.C. Mundekkad, Cho, Nanoparticles in clinical translation for cancer therapy, Int. J. Mol. Sci. 23 (2022) 1685.

[68] R. Preet, P. Mohapatra, S. Mohanty, S.K. Sahu, T. Choudhuri, M.D. Wyatt, C. N. Kundu, Quinacrine has anticancer activity in breast cancer cells through inhibition of topoisomerase activity, Int. J. Cancer. 130 (2012) 1660–1670.

[69] M. Sharifi-Rad, Y.K. Mohanta, P. Pohl, D. Nayak, M. Messaoudi, Facile phytosynthesis of gold nanoparticles using *Nepeta bodeana* Bunge: Evaluation of its therapeutics and potential catalytic activities, J. Photochem. Photobiol., a. 446 (2024), 115150.

[70] H.S. Elshafie, M.F. Armentano, M. Carmosino, S.A. Bufo, V. De Feo, I. Camele, Cytotoxic activity of *Origanum vulgare* L. on Hepatocellular carcinoma cell line HepG2 and evaluation of its biological activity, Molecules 22 (2017) 1–16.

[71] J.M. Calderón-Montaño, S.M. Martínez-Sánchez, V. Jiménez-González, E. Burgos-Morón, E. Guillén-Mancina, J.J. Jiménez-Alonso, P. Díaz-Ortega, F. García, A. Aparicio, M. López-Lázaro, Screening for selective anticancer activity of 65 extracts of plants collected in western Andalusia, Spain, Plants. 10 (2021) 2193.

[72] M. Mahiuddin, P. Saha, B. Ochiai, Green synthesis and catalytic activity of silver nanoparticles based on *Piper chaba* stem extracts, Nanomaterials, 10 (20209)1777.

[73] L. Xu, X.C. Wu, J.J. Zhu, Green preparation and catalytic application of Pd nanoparticles, Nanotechnology 19 (2008), 305603.

[74] J. Saha, A. Begum, A. Mukherjee, S. Kumar, A novel green synthesis of silver nanoparticles and their catalytic action in reduction of Methylene Blue dye, Sustain, Environ. Res. 27 (2017) 245–250.